

Morphological and thermal properties of PLA/OMMT nanocomposites prepared via vane extruder

Y Luo¹, H Y Liu¹, G Z Zhang¹ and J P Qu^{1,2}

¹National Engineering Research Center of Novel Equipment for Polymer Processing, The Key Laboratory of Polymer Processing Engineering of Ministry of Education, South China University of Technology, Guangzhou 510640, China

E-mail: jpqu@scut.edu.cn

Abstract. Polylactide/Organo-Montmorillonite (PLA/OMMT) Nanocomposites were prepared by melting extrusion using a novel vane extruder (VE), which can induce global elongational flow. In the study, the influence of different concentrations of the OMMT on the morphological and thermal properties were investigated. The morphology and structure of the nanocomposites were evaluated using Fourier Transform Infrared Spectroscopy (FTIR), the X-ray diffraction (XRD) and transmission electron microscopy (TEM) respectively, whereas the thermal behaviors and thermal stabilities were characterized using differential scanning calorimetry (DSC) and thermal gravimetric analysis (TGA) respectively. The results illustrate that PLA/OMMT nanocomposites displayed clear intercalation and/or exfoliation structures. Interestingly, increasing the clay content did not lead to the agglomeration of OMMT layers. Moreover, the presence of nanoclay decreased the enthalpy of crystallization of PLA/OMMT composites. Also, the melting temperatures of the nanocomposites were reduced by the addition of nanoclay.

1. Introduction

Recently, biodegradable and biocompatible polymers have attracted tremendous attention both from biomedical and ecological possibility [1]. PLA, one of such polymer, has superb properties such as biocompatibility, thermal plasticity, high strength and stiffness, so there is a large prospect of developing PLA as ideal substitutes for the petrochemical plastics in polymer applications [2-3]. However, its drawbacks, such as low heat distortion temperature and inferior hydrophobicity, limit its use in various end-use applications [4]. In spite of the dissatisfaction, many considerable attempts have been carried out to enhance these properties [5-6].

In recent decades, the incorporation of nanoclay into the PLA matrix has received considerable interest as one of the most universally approved and feasible measures, since significant improvements in properties are observed at lower clay content. Besides that, clay materials are easily obtainable, environmentally harmlessly. Forming a kind of delamination and/or exfoliation structure of nanoclay in PLA matrix is necessary for preparing superior nanocomposites. Because the synergistic effects of the nanoscale structure and the interaction of the fillers and polymer matrix perhaps can improve some properties. Several processing methods have been considered to prepare PLA-layered silicates for the superstructure and micromorphology of PLA in situ intercalative polymerization [7], solvent intercalation [8-9] and direct melt intercalation [5-6, 10-11] using a polymer mixer or screw extruder. Ogata et al. [8] first prepared PLA organically modified clays blends by the solvent-cast method.



Sinha Ray et al. [11] prepared PLA/clay nanocomposites with a twin screw extruder and the intercalated structure of silicate layers of the clay was observed, it was revealed that clay randomly distributed in the PLA matrix. Okamoto [12] studied a range of PLA-based systems differing from the OMMT in the aspect ratio of the nature of the organic modifier. The results indicated that PLA/clay could possess an excellent enhancement in physical as compared with the pure PLA matrix.

However, all these improvements are based on classic screw extruder and there are some disadvantages of polymer composites prepared by a conventional extruder which is based on the shear flow. In polymer processing, the shear flow is less efficient than the elongation flow. More specially, according to some researchers, it is relatively effective to crush the melt drops under elongation flow rather than under shear flow [13-14]. Given that the incorporating of strong elongation flow has a good prospect on nanocomposite processing, a novel vane extruder (VE) will particularly be used in this study. Qu. [15] designed the VE, which can induce a global elongation flow. Moreover, the vane extruder shows a short thermo-mechanical history and wide suitability in polymer processing, hence the vane extruder can reduce particle size and macromolecule chain broken. From our previous experiments, finer dispersion particles and well mechanical properties have been obtained using VE because of its positive displacement-type characteristics [16-18], and the comparison between VE and traditional extruder has been researched in our previous works [16,18-19].

The aim of this study is to evaluate the effectiveness of OMMT concentration on dispersion, morphological, and thermal properties of PLA/OMMT composites prepared by elongation flow. In this way, it can offer a theoretical background to understand the nanocomposite formation in VE.

2. Experimental

2.1. Materials

Poly(lactide) (PLA 3051D, density=1.24g/cm³) was obtained from NatureWorks. Its glass transition temperature (T_g) and melting temperature (T_m) were 62°C and 164°C, respectively. The melt flow index of the PLA was 25g/10 min (2.16 kg load, 210°C). Montmorillonite clay (1.34 TCN, Nanocor density = 2.00g/cm³) was modified with methyl dihydroxyethyl hydrogenated tallow ammonium.

2.2. Preparation of PLA/OMMT nanocomposites

PLA/OMMT nanocomposites were prepared by a novel vane, whose schematic diagram is showed in Figure 1. Clearly, a number of groups of Vane Plasticating and Conveying Units (VPCUs) constitute the vane extruder. One group of VPCUs is made up of a rotor, a stator, two baffles and four vanes. Obviously, there are four cylindrical chambers between two baffles along the axial direction of the rotor. The polymer will be fed into the first VPCU and subsequently discharged into the next VPCU via the hole in the baffle, as the volume of chamber ranges from the maximum to minimum periodically. Simultaneously, materials get the necessary heat from the external heating and particulate deformation. It indicates that an elongational flow is induced by the volume transportation. Three different formulations including 2.5wt%, 5wt% and 7.5wt% OMMT fillers in the PLA matrix were fabricated by VE. Neat PLA pellets were prepared under the same conditions to get a reference material (the same thermal history). Before compounding, 8 hours' drying process was carried to PLA and OMMT in a vacuum oven at 80°C. Then PLA and OMMT clay were put into a dry plastic zip-lock bag, rolling over the bag to mix the materials and afterward feeding into the VE for melt-processing. The temperature setting of four zones from the hopper to die were 175-180-195-195°C, the rotor speed was set at 60rpm. The extruded composites were cooled naturally and subsequently pelleted by a granulator. The test samples for TEM were compression molded in a hydraulic press at 200°C for 30 min, which were in the form of 150×80×4mm³. The samples for XRD, DSC and TG characterization were obtained from the fresh extruder at the exit of the die. The films samples (0.4mm thickness) for FTIR test were hot compressed from the extruder molded plaques.

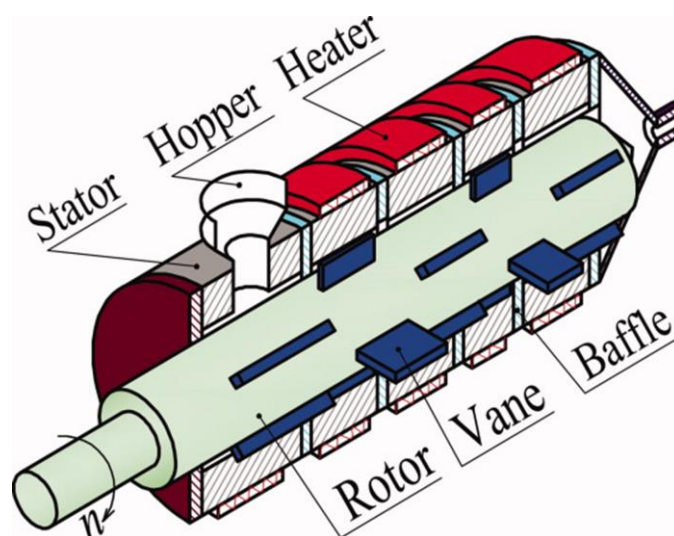


Figure 1. Schematic diagram of the vane extruder.

Table 1. Main parameters of vane extruder.

Main parameter	Value(mm)
Number of VCPUS	19
Radius of rotator	40
Internal radius of stator	48
Aspect ratio of rotator axis	10
Eccentricity distance	4

2.3. Characterization

X-ray diffraction (XRD) experiments were conducted to measure the d-spacing of the OMMT clay and the clay in the PLA/OMMT nanocomposites on a Germanic diffractometer (D8 ADVANCE), operating at the X-ray radiation (wave strength $\lambda = 0.15418$ nm, 40 KV and 40 mA). The mass of each sample include pure OMMT and PLA/OMMT nanocomposite with 2.5wt%, 5wt% and 7.5wt% are kept the same for measuring the d-spacing of OMMT layers in samples. The measurement was performed at a 2θ range of $2-30^\circ$, a scanning step of 0.02° , and a scanning rate of $2^\circ/\text{min}$.

Transmission electron microscopy (TEM: A Philips TECNAL 10) was used to characterize the dispersion of OMMT in the PLA/OMMT at an accelerated voltage of 120kV. The ultrathin sections for the TEM characterization were obtained from the samples by a Powertome X (Boeckeler Instrument) cryo-ultramicrotome.

Fourier Transform Infrared Spectroscopy (FTIR) analysis was conducted using an American instrument (Nexus 670, Nicolet Company). The spectra from $500-4000\text{ cm}^{-1}$ were recorded with an absorption of 32 scans.

Differential scanning calorimetric (DSC) measurements were carried out via a Netzsch DSC204 (Germany) under the nitrogen atmosphere. All test samples of 5-10 mg were heated from room temperature to 230°C at a rate of $10^\circ\text{C}/\text{min}$ and maintained 10 min, and then cooled -70°C , hold for 10 min. Lastly, these specimens were heated to 230°C .

Thermo-gravimetric analysis (TGA) of the samples were performed on an instrument (TG209, NETZSCH) at a heating rate of $20^\circ\text{C}/\text{min}$ under a flow of N_2 , from the room temperature to 700°C . TGA analyses were repeated in the air.

3. Results and discussion

3.1. Interactions between PLA and nanoparticles

The FTIR spectrum of PLA and PLA/OMMT nanocomposites was presented in Figure 2. It is noteworthy that the 1000-3130 cm^{-1} spectrum is omitted because there is no change in the range. The peaks at 3700-3400 cm^{-1} are ascribed to the OH stretching of the $-\text{CH}(\text{CH}_3)-\text{OH}$ end group of PLA. The peaks at 3700-3590 cm^{-1} , 3590-3300 cm^{-1} are assigned to the free hydroxyl and hydroxyl. The intensity of the free hydroxyl peak enhances with the loading of silicate clay, and the peak position shifts to lower wavenumbers. Interestingly, the position of associating hydroxyl do not change, and the intensity increases with the OMMT loading. The strong interactions between the hydroxyl of PLA end groups and OMMT lamella surfaces and/or the hydroxyl groups of the surface active agent in the OMMT fillers have caused above phenomenon.

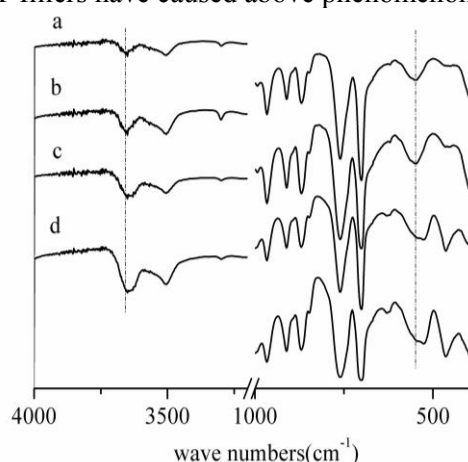


Figure 2. FTIR spectrum of Pure PLA and PLA/OMMT nanocomposites, (a) Pure PLA, (b) PLA/OMMT (2.5wt %), (c) PLA/OMMT (5wt %), (d) PLA/OMMT (7.5wt %).

3.2. Interactions between PLA and nanoparticles

3.2.1. X-ray Diffraction (XRD). Figure 3 presents the XRD patterns of montmorillonite clay and PLA/OMMT nanocomposites. In Figure 3, log scale was used to compare the peaks near 5 degree more clearly. It indicates that there exists OMMT nanofiller intercalation and/or exfoliation in diverse PLA/OMMT nanocomposites. The order diffraction (001) of neat OMMT clay is registered at $2\theta = 4.84^\circ$, which means a basal spacing of 1.83nm, according to Bragg's law ($\lambda = 2d \sin \theta$; λ is the X-ray wavelength; d is the layer spacing). In the PLA/OMMT nanocomposites, 2θ of the (001) diffractions shifts to a higher angle for the composites of 2.5wt% (5.34°), 5wt% (5.05°) and 7.5wt% (5.00°) and the corresponding gallery spacing decreases than that of neat OMMT, as displayed in Table 2. This change is attributed to the elongational flow field which can break the homogeneous OMMT layers [20]. Also, the strong interplay between the PLA and the modified OMMT layer is another factor. The preservation of the peak (001) in the blends reveals that a portion of OMMT with the lamellar structure still maintains after the melt blending process despite part of OMMT may be intercalated and/or exfoliated in diverse PLA/OMMT blends.

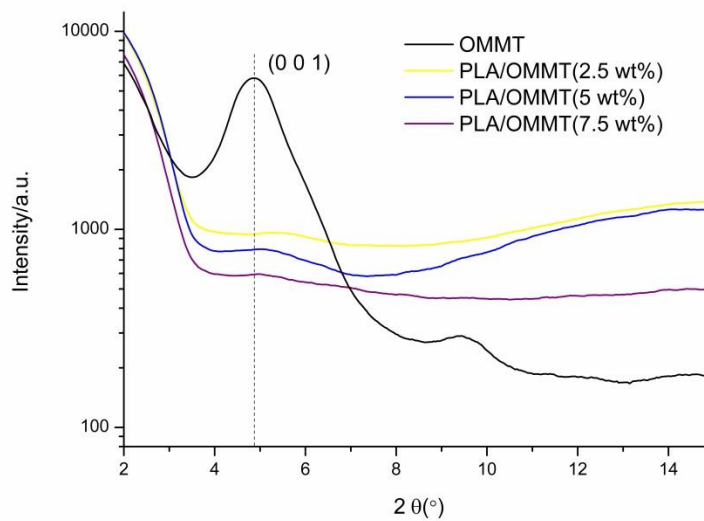


Figure 3. XRD patterns for OMMT and PLA/OMMT nanocomposites.

Table 2. D-spacing of OMMT and PLA nanocomposites.

Samples	$2\theta(^{\circ})$	d-spacing (\AA)
OMMT	4.84	18.3
PLA/OMMT (2.5 wt %)	5.34	16.5
PLA/OMMT (5 wt %)	5.05	17.4
PLA/OMMT (7.5 wt %)	5.00	17.7

3.2.2. Transmission Electron Microscopy (TEM). Figure 4 displays the micrographs of PLA/OMMT nanocomposites. In Figure 4, the light regions are identified as PLA matrix, and the deep linear objects are piles of OMMT crystal lamellar. As showed in the Fig 4a-c, portions of the OMMT platelets successfully intercalate into the PLA/OMMT compounds. It indicates that the intercalated and/or exfoliated structure coexisted. Moreover, at high particle concentration (7.5wt%), the PLA matrix penetrates the OMMT layers, promoting the exfoliation of OMMT, as complete separation of the montmorillonite nanoclay by PLA chains. Interestingly, there is no agglomeration in the composites (Figure 4c), which corresponded to the XRD analysis. It is indicated that there are presentable dispersion and distribution of OMMT nanofiller in PLA matrix at various contents, which can be ascribed to the high pressure stressed of the polymer melt during processing in VE and the ammonium surfactant in the OMMT particle.

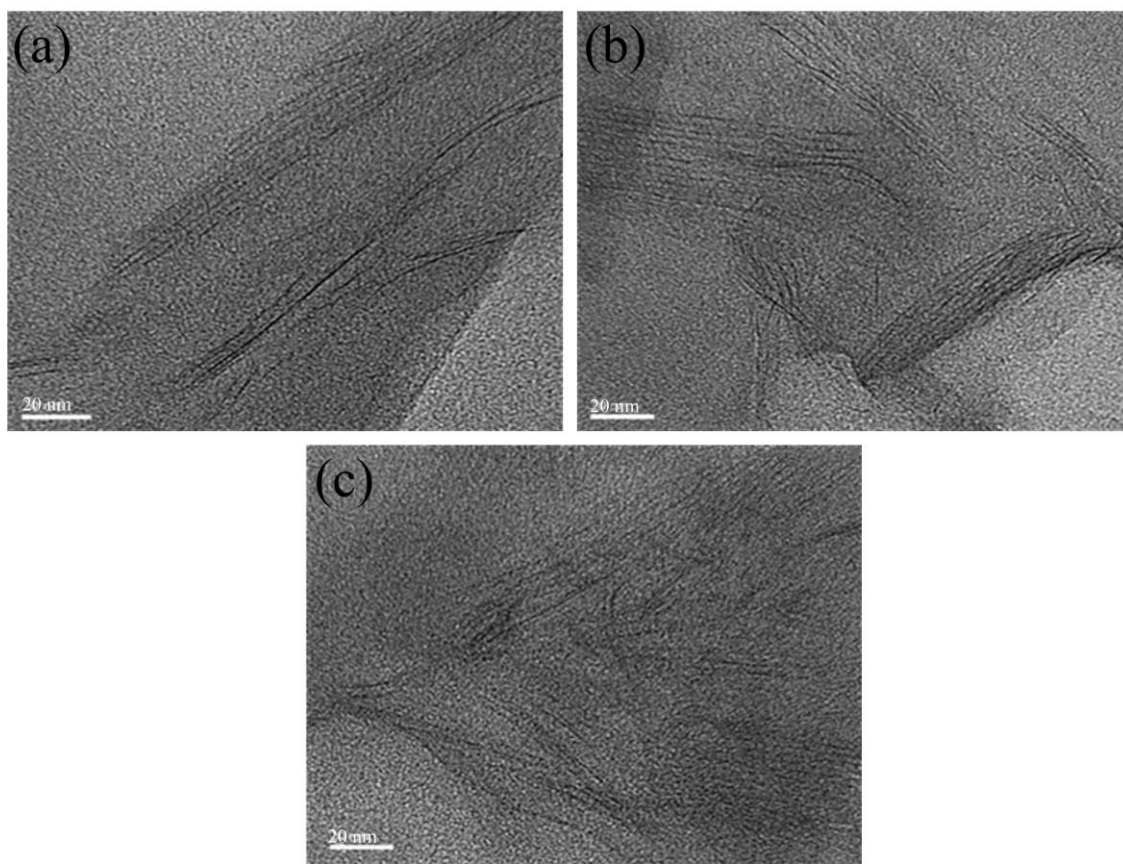


Figure 4. TEM micrographs of PLA nanocomposites with OMMT: (a) 2.5wt% OMMT, (b) 5wt% OMMT, (c) 7.5wt% OMMT.

3.3. Thermal analysis

3.3.1. Crystallization and melting behavior. The DSC thermograms of PLA and PLA/OMMT blends in the first cooling scan after rapid heating at 10°C/min are presented in Figure 5. All thermodynamic parameters can be calculated from the curves, as showed in Table 3. It can be found that the increasing of OMMT concentration decreases the glass transition of PLA (62.4°C) from Table 3. In Figure 5, we can see that the crystallization peak of PLA is found at the peak temperatures about 118.9°C in the crystallization curve. However, the crystallization temperatures of PLA/OMMT nanocomposites decreases at different extent compared to neat PLA. These findings confirm that when rapidly cooled from the molten state, PLA/OMMT nanocomposites are inadequate for crystallization. Moreover, the enthalpy of crystallization of PLA matrix decreases with the loading of OMMT nanofillers. It can be considered that there is a good interplay between PLA matrix and OMMT fillers and large surface areas and volume ratios of the OMMT clays [21]. DSC melting thermograms of PLA and its nanocomposites in the second heat scan after rapidly cooling from the molten situation are presented in Figure 6. In Figure 6, a melting peak at 153°C (T_{m1}) with a shoulder at 163.0°C (T_{m2}), and a cold crystallization peak as well are observed. However, the addition of OMMT transforms these peaks into two separated melting peaks and there are no cold crystallization peaks. Since the imperfect crystals have sufficient time to melt and recombine into crystals with higher structure perfection, and remelt at a higher temperature [21]. Simultaneously, the relatively small melting peak overlap with the crystallization peak, thus the melting of polymer is took place in parallel with the stacking and crystallization of molecular chain. The energy released by the crystallization has been counterbalanced, because the melting rate is greater than the rate of crystallization, and the energy required for melting is greater than the energy released by the crystallization. Thus it is observed of this independent bimodal melting peak in the melting curve of PLA/OMMT nanocomposites. Additionally, the

incorporation of OMMT clay induces a clear decrease of the melting temperature of neat PLA (153°C), implying the OMMT fillers can promote the crystallization ability of PLA matrix. Especially, the largest degree of decline of the melting temperature of PLA is occurred in the PLA/OMMT blend with 2.5wt% nanofillers owing to the stronger interaction between organic surfactant of OMMT and the functional groups of PLA chains.

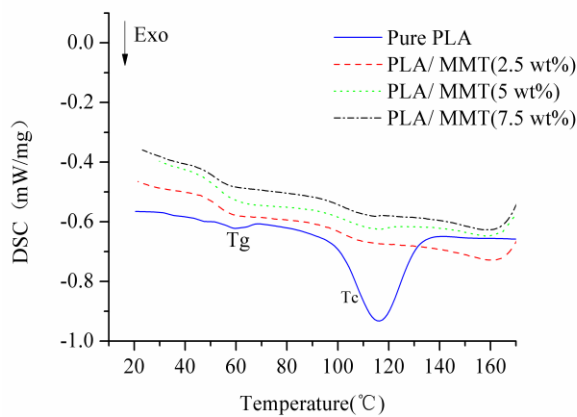


Figure 5. Crystallization curves of PLA and PLA/OMMT nanocomposites.

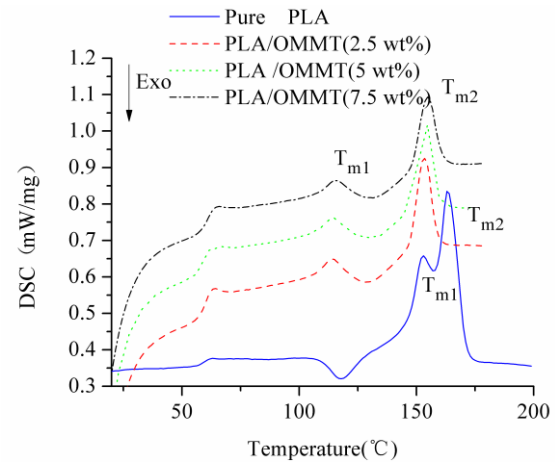


Figure 6. Melt curves of PLA and PLA/OMMT nanocomposites.

Table 3. Characteristic thermal properties of PLA and PLA/OMMT nanocomposties.

OMMT (wt %)	T _g (°C)	T _c (°C)	T _{m1} (°C)	T _{m2} (°C)
0 (Pure PLA)	62.4	118.9	153.0	163.3
2.5	60.8	110.1	113.9	153.5
5	57.6	115.2	114.2	154.7
7.5	56.3	112.7	115.2	154.8

T_g: the glass transition temperatures, T_c: cold crystallization temperature, T_{m1}, T_{m2}: the melting temperatures of PLA.

3.3.2. Thermal Gravimetric Analysis (TGA). Thermo-gravimetric analysis was made to study the thermal degradation characteristics of PLA/OMMT blends. Generally, the nanocomposite has most of weight losses in the region of 300-600°C. Figure 7 presents the TGA curves of PLA and PLA/OMMT nanocomposites. The initial degradation temperatures (T_d , at 10% weight loss), the degradation temperature at 50% weight loss ($T_{50\%}$) and the weight of the residue at 600°C (ω_t^{600}) are shown in Table 4. From the curves and the table, the T_d of the PLA/OMMT blends increases slightly with the loading of OMMT, suggesting that the incorporation of silicate nanofiller into PLA matrix can cause an enhancement of the thermal stabilities of the polymer matrix. The ω_t^{600} increases gradually with the increasing clay loadings of OMMT. This result can be explained by the good thermal stability of OMMT and to the interaction between the polymer matrix and the clay particles. Moreover, this changing tendency of the ω_t^{600} with the OMMT concentration is ascribed to the high heat resistance exerted by the OMMT clay itself. Similar phenomenon was also reported by some researchers [22-23]. In addition, the $T_{50\%}$ increases gradually with the clay content with a maximum increase of 29°C from the value of neat PLA (373°C for the 5wt% OMMT and of 26°C, 23°C for the 2.5wt%, 7wt% respectively). With increasing of OMMT concentration, a slight decrease has been eyed in the nanocomposites based on 7.5wt% clay loadings. Such phenomenon can be explained by that increasing the incorporation of OMMT silicate nanofiller into PLA matrix results in relatively more exfoliated particles and enhances the thermal stabilities of the PLA/OMMT blends.

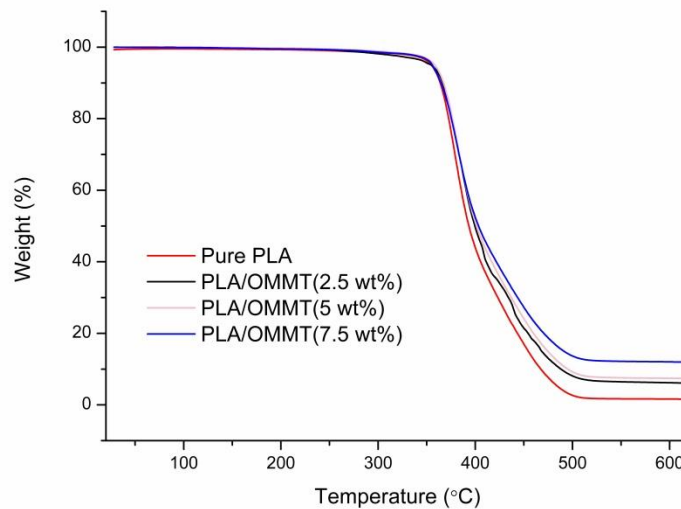


Figure 7. TGA thermograms for PLA and PLA/OMMT nanocomposites.

Table 4. TGA for PLA and PLA/OMMT nanocomposites.

OMMT (wt %)	T_d (°C)	$T_{50\%}$ (°C)	ω_t^{600} (%)
0 (Pure PLA)	365	373	0.22
2.5	369	399	6.49
5	372	402	7.53
7.5	368	396	12.20

4. Conclusions

PLA/OMMT nanocomposites with different OMMT content were successfully prepared by melt-blend using a novel VE. The effect of OMMT concentration on morphological, thermal properties of the PLA/OMMT blends has been discussed. Morphological studies show that intercalation/ exfoliation structure in the PLA matrix was revealed, and good dispersions of OMMT nanoparticles were observed in all samples with various OMMT concentrations. The results can be explained by the high elongation stressed of the polymer melt in vane extruder. Also with the loading of OMMT increases, the crystallization ability of the blends enhanced. Furthermore, it is indicated that the incorporation of OMMT clay enhanced the thermal stability of PLA/OMMT nanocomposites, thus, providing the possibility of application of PLA/OMMT composites at a higher temperature than pure PLA.

Acknowledgments

We acknowledge the National Natural Science Foundation of China (Grant No. 51435005, 51505153), PhD Start-up Fund of Natural Science Foundation of Guangdong Province, China (Grant No. 2016A030310429), the Special-funded Program on National Key Scientific Instruments and Equipment Development of China (Grant No. 2012YQ230043) and Science and Technology Program of Guangzhou, China (Grant No.201607010240) for financial support.

References

- [1] Bordes P, Pollet E and Avérous L 2009 *Prog. Polym. Sci.* **2** 125
- [2] Rasal R M and Hirt D E 2009 *Macromol. Biosci.* **9** 989
- [3] Zhang Z and Feng S S 2006 *Biomaterials* **27** 4025
- [4] Rasal R M, Janorkar A V and Hirt D E 2010 *Prog. Polym. Sci.* **35** 338

- [5] Nam P H, Fujimori A and Masuko T 2004 *J. Appl. Polym. Sci.* **93** 2711
- [6] Pluta M, Galeski A, Alexandre M, Paul M A and Dubois P 2002 *J. Appl. Polym. Sci.* **86** 1497
- [7] Cao H, Wang P, Yuan W and Lei H 2010 *J. Appl. Polym. Sci.* **115** 1468
- [8] Ogata N, Jimenez G, Kawai H and Ogihara T 1997 *J. Polym. Sci., Part B: Polym. Phys.* **35** 389
- [9] Wu T M and Wu C Y 2006 *Polym Degrad Stabil.* **91** 2198
- [10] Jonoobi M, Harun J, Mathew A P and Oksman K 2010 *Compos. Sci. Technol.* **70** 1742
- [11] Nam J Y, Ray S S and Okamoto M 2003 *Macromolecules.* **36** 7126
- [12] Ray S S and Okamoto M 2003 *Prog. Polym. Sci.* **28** 1539
- [13] Tokihisa M, Yakemoto K, Sakai T, Utracki L A, Sepehr M, Li J and Simard Y 2006 *Polym. Eng. Sci.* **46** 1040
- [14] Scott C E and Macosko C W 1991 *Polym. Bull.* **26** 341
- [15] Qu J P 2008 *C.N. Patent* 200,810,026,054.X
- [16] Jia S K, Qu J P, Wu C R, Liu W F, Chen R Y, Zhai S F, Huang Z and Chen F Q 2013 *Langmuir* **29** 13509
- [17] Qu J P, Zhang G Z, Chen H Z, Yin X C and He H Z 2012 *Polym. Eng. Sci.* **52** 2147
- [18] Qu J P, Zhao X Q, Li J B and Cai S Q 2013 *J. Appl. Polym. Sci.* **127** 3923
- [19] Jia S, Qu J P, Zhai S, Huang Z, Wu C R, Chen R Y and Feng Y H 2014 *Polym. Compos.* **35** 884
- [20] Ray S S, Okamoto K and Okamoto M 2003 *Macromolecules* **36** 2355
- [21] Jiang L, Zhang J and Wolcott M P 2007 *Polymer* **48** 7632
- [22] Chang J H and An Y U 2002 *J. Polym. Sci. B Polym. Phys.* **40** 670
- [23] Chang J H, An Y U and Sur G S 2003 *J. Polym. Sci. B Polym. Phys.* **41** 94